

Nanoindentation Studies of the MBE-Grown, Zero-Gap (Hg,Cd)Te Epilayers

R. MINIKAYEV^a, S. ADAMIAK^b, A. KAZAKOV^c, E. ŁUSAKOWSKA^a, R. KUNA^a,
J. GRENDYSA^b, E.M. SHEREGII^b, T. WOJTOWICZ^c AND W. SZUSZKIEWICZ^{a,b,*}

^aInstitute of Physics, Polish Academy of Sciences, Aleja Lotników 32/46, PL-02668 Warsaw, Poland

^bFaculty of Mathematics and Natural Sciences, University of Rzeszów,
S. Pigoń 1, PL-35310 Rzeszów, Poland

^cInternational Research Center MagTop, Institute of Physics, Polish Academy of Sciences,
Aleja Lotników 32/46, PL-02668 Warsaw, Poland

(Hg,Cd)Te epilayers containing a dozen percent of CdTe were grown by molecular beam epitaxy technique on GaAs wafers with thick CdTe buffer layers. The X-ray diffraction method was used to determine a chemical composition of the epilayers. The scanning electron microscopy measurements in turn were performed to determine the thickness of epilayers, and both scanning electron and atomic force microscopy to evaluate structures' morphology. The selected mechanical properties of samples were studied by the nanoindentation technique. The average values and standard deviations of the nanohardness and Young's modulus were extracted from the collected load-displacement data. The values of both parameters were compared with those determined for bulk crystals and those known from the literature.

DOI: [10.12693/APhysPolA.136.603](https://doi.org/10.12693/APhysPolA.136.603)

PACS/topics: 62.20.-x

1. Introduction and motivation

The ternary HgCdTe alloys form a continuous series of (Hg,Cd)Te solid solutions with CdTe content ranging from 0 to 100%. All of them possess zinc blende crystal structure [1]. The crystals containing up to about 30% of CdTe belong to the class of narrow-gap semiconductors. For a low CdTe content these crystals exhibit an inverted band structure, and the zero-energy gap at liquid helium temperature is achieved in (Hg,Cd)Te containing around 15% of CdTe [1]. This inverted band structure of the solid solution is characterized by the linear dependence of conduction band energy on wave vector. Thus, according to the Kane theory describing the band structure of a narrow-gap semiconductor [2], the electron effective mass at the conduction band edge is exactly zero. Many physical properties of the (Hg,Cd)Te are strongly affected by its unique band structure. It concerns not only the electron transport, but also the interband or free-carrier absorption [3], optical phonon modes [4], etc. The narrow-gap (Hg,Cd)Te was intensively investigated from the sixties of last century and many review papers, chapters in books or whole monographs were dedicated to various properties of this solid solution (for details see [1, 5, 6] and references therein). The (Hg,Cd)Te crystals found several important applications, in particular for making optical devices working in the infrared spectral range of radiation [6]. Over the last years (Hg,Cd)Te

with an inverted band structure has again attracted a lot of attention due to its possible transition from a normal to a topological insulator phase [7] and the first observation of the quantum spin Hall effect [8]. It is believed that the materials with the massless Dirac fermions having a linear momentum-energy relationship and forming a new class of quantum matter, can find a number of novel applications that will be based on their unique physical properties.

Recently, it was demonstrated that selected mechanical properties of PbTe bulk crystals and molecular beam epitaxy (MBE)-grown PbTe layers differ substantially [9]. In the case of GaAs, however, the analogous difference seems to be much smaller [10]. Therefore, an interesting question arises whether this effect exists also in II-VI semiconducting compound. The (Hg,Cd)Te solid solution seems to be an excellent object for such investigations.

The aim of present study is to determine the nanohardness and Young's modulus of (Hg,Cd)Te solid solution by the method of nanoindentation. The alloy compositions similar to these corresponding to the energy band inversion, were selected for this purpose.

2. Experimental details

(Hg,Cd)Te layers, approximately 1 μm thick, containing a dozen percent of CdTe were grown by the MBE technique at the Centre for Microelectronics and Nanotechnology of the University of Rzeszów. The Double RIBER COMPACT 21 system was used for the growths. First, the (001)-oriented or slightly misoriented (of the order of one degree) GaAs wafers (from AXT company)

*corresponding author; e-mail: szusz@ifpan.edu.pl

were overgrown with CdTe buffers of the thickness from 3 to 4 μm . Next, the (Hg,Cd)Te solid solution layers with thickness ranging from approximately 300 to 1000 nm and chemical compositions not exceeding 20% of CdTe were grown on hybrid substrates prepared in such a manner. For more details on the growth technology see [11, 12].

The (Hg,Cd)Te layer thickness was determined by scanning electron microscopy (SEM) while the surface morphology was evaluated by both SEM and atomic force microscopy (AFM). Prior to the nanoindentation measurements the structural characterization and the determination of chemical composition of all crystals was performed with the use of X-ray diffraction (XRD) technique. The X-Pert PANanalytical X-ray diffractometer and Cu K_{α_1} radiation was used and the X-ray diffraction pattern was measured in a wide angular range ($10^\circ \leq 2\theta \leq 150^\circ$). For the nanoindentation measurements the Ultra Nanohardness Tester CSM UNHT/AFM was used with the following parameters: maximum load 0.5 mN, linear change of the load vs. time during application or removal of the load 0.033 mN/s, application time of the maximum load 15 s. The average values and standard deviations of the nanohardness and Young's modulus were extracted from the determined load–displacement relation.

The bulk (Hg,Cd)Te crystals used for a comparison were grown by the Bridgman method and their chemical composition was verified by XRD.

3. Results and discussion

The typical results of XRD measurements for both types of samples are shown in Fig. 1 and Fig. 2. Figure 1 presents a part of X-ray diffraction pattern obtained for the (Hg,Cd)Te epilayer which was grown on slightly misoriented (001)-GaAs substrate. The perfect epitaxial character of the (Hg,Cd)Te layer and its (001) orientation can be seen. Very small intensity of the structure corresponding to a contribution from (111)-oriented (Hg,Cd)Te indicates a residual character of this crystal phase. The lattice parameter of the solid solution, resulting from the measured diffraction pattern, is equal to 6.4642 Å. Taking into account the lattice parameter for HgTe ($a = 6.4604$ Å) [13] and for CdTe ($a = 6.481$ Å) [14] and assuming the Vegard relation, one can obtain that the (Hg,Cd)Te layer contains about 19% of CdTe. Figure 2 presents the diffraction pattern measured for the layer grown on exactly oriented (001) GaAs substrate. This pattern clearly indicates a polycrystalline character of the growth. The relevant lattice parameter is slightly higher and the layer contains a few percent more CdTe than the previous one. The dependence of the crystallographic structure of MBE grown layers on the misorientation of GaAs substrate is a well-known phenomenon and it was observed previously not only for a number of II–VI semiconducting compounds and their solid solutions, but also for many other materials

(e.g., for zinc blende MnTe [15]). Since values of the CdTe and (Hg,Cd)Te lattice parameters are similar, the Bragg peaks that have been obtained from diffraction on both layers grown by MBE, resulted in being very close to each other. They are not well separated as can be seen in Fig. 1 and Fig. 2.

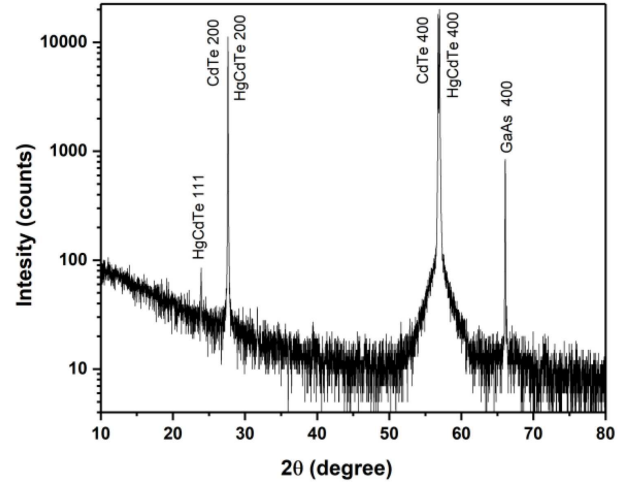


Fig. 1. The typical XRD pattern of the structure grown on slightly misoriented (001) GaAs substrate with CdTe buffer.

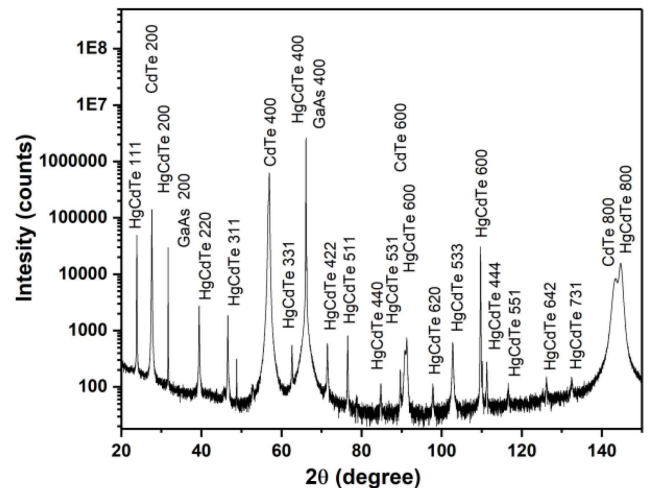


Fig. 2. The typical XRD pattern of the structure grown on (001)-oriented GaAs substrate with CdTe buffer.

The Raman scattering can in principle serve for an independent estimation of a chemical composition of a solid solution. It is because the frequency position of structures related to scattering of optical phonons changes with varying composition. Although the previously determined frequency position of the Raman structures for the (Hg,Cd)Te solid solution can be found in the literature, e.g., in [16], the estimation of composition with the use of the Raman studies is not an easy task due to a number of complications mentioned below.

The phonon excitations for (Hg,Cd)Te exhibits two-mode behavior due to a significant difference of mass of constituent metal atoms. One can also expect an appearance of a subtle structure of transversal optic (TO) phonon modes. It can result from a number of possible, different distributions of Hg and Cd ions on lattice sites around the Te ion, forming a deformed tetrahedron. In fact, the far-infrared reflectivity spectra taken on (Hg,Cd)Te bulk samples have demonstrated a complex structure of observed TO modes which result from this effect (see [17, 18] and references).

One has to mention also that for a small power of laser excitation (a few mW only) that corresponds to a really small intensity of the Raman scattering signal and a high noise level, the MBE-grown (Hg,Cd)Te layers can be easily damaged during experiment. As a result of this degradation process, the hexagonal tellurium precipitates are formed. Now, efficiency of the Raman scattering on crystalline Te is very high and the presence of even a small number of Te precipitates in investigated material can lead to additional Raman structures in the interesting frequency range [19]. Therefore, the Raman spectroscopy seems to be not the best experimental tool to determine (Hg,Cd)Te chemical composition precisely. Therefore, this method was not applied in the present study.

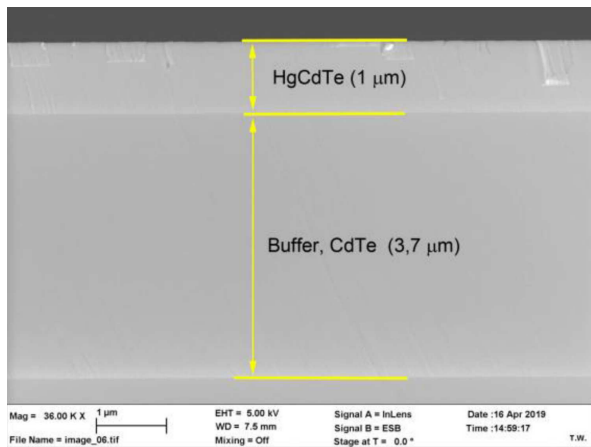


Fig. 3. The side view of the structure of Fig. 1 obtained by SEM.

Figure 3 shows the side view of the sample presented in Fig. 1, and taken by SEM: the thickness of CdTe buffer was approximately $3.7 \mu\text{m}$ and that of the (Hg,Cd)Te close to $1 \mu\text{m}$. The surface of this sample investigated by AFM is shown in Fig. 4. The analyzed surface area was $20 \mu\text{m} \times 20 \mu\text{m}$, and the estimated surface roughness (RMS) was $\approx 2.3 \text{ nm}$.

The result of nanoindentation measurement performed for the sample under discussion and its interpretation are shown in Fig. 5 and Fig. 6. In order to measure properties of an epitaxial layer alone (avoiding possible influence of a substrate), the indentation depth should be

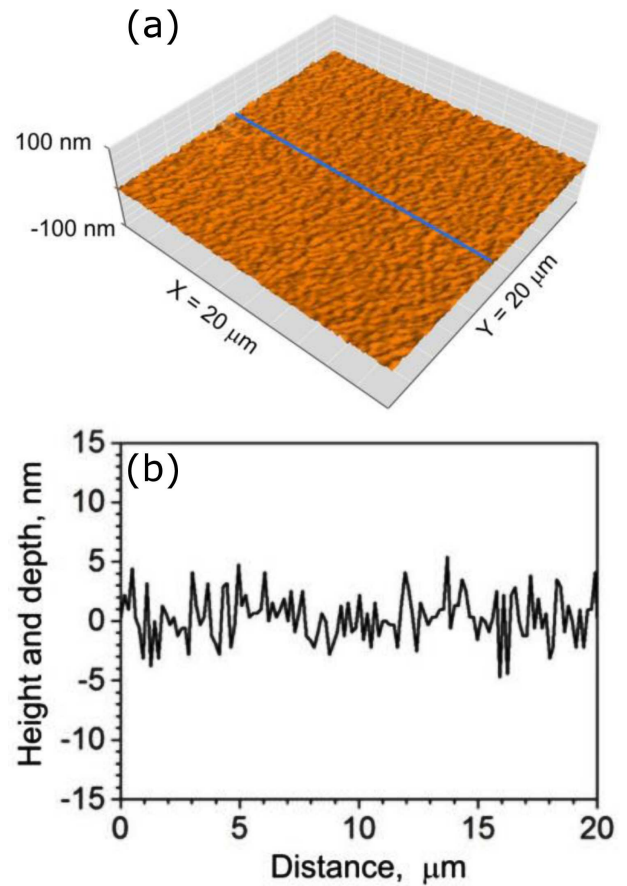


Fig. 4. The result of AFM measurements of the (Hg,Cd)Te layer shown in Fig. 1 and Fig. 3. (a) Surface topography of the layer, (b) Surface profile along the line indicated in (a).

kept within several percent of the layer thickness. This value should be from 10 to 20% (see [9] and references). Importantly, the MBE-samples studied here satisfied this condition. The nanohardness values $H = (550 \pm 40) \text{ MPa}$ and Young's modulus values $E = (53 \pm 3) \text{ GPa}$ were determined. These values are in an agreement with experimental data [20] for MBE-grown (Hg,Cd)Te layer containing 30% of CdTe, in spite of dealing with different composition. Values obtained in [20] are $H = 660 \text{ MPa}$ and $E = 42 \text{ GPa}$. The difference between our present values and that are reported in [20] comes from hardening of the soft HgTe material with an increasing Cd content. This effect is well known for bulk (Hg,Cd)Te solid solutions [21–27], and was also observed for (Hg,Zn)Te solid solutions [23, 25]. More recently similar effect was observed for PbTe, relatively soft material belonging to the group of IV–VI semiconducting compounds. The results were reported for (Pb,Cd)Te solid solution [28, 29].

The mechanical properties of zinc blende crystals are in general anisotropic and materials are stiffer along $\langle 111 \rangle$ body diagonal [30]. However, the hardness values determined for [001]-type direction are only a couple of percent smaller than that for [011]-type crystal direction for

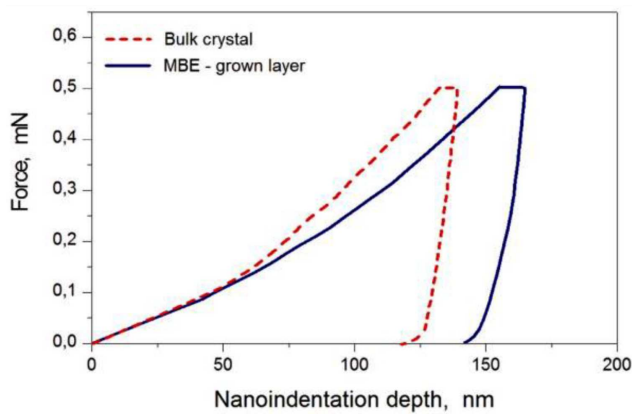


Fig. 5. The applied load–nanoindentation depth experimental curves obtained for MBE-grown layer from Fig. 1 and the bulk crystal with the same chemical composition.

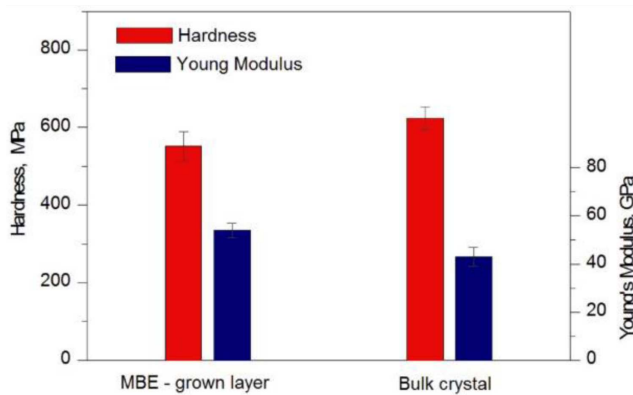


Fig. 6. The comparison of the nanohardness and Young's modulus values resulting from nanoindentation measurements shown in Fig. 5.

tetrahedrally coordinated materials [31]. Therefore, the results of nanoindentation measurement on MBE grown (001)-oriented (Hg,Cd)Te layer can be compared with those determined for the (011)-oriented, solid solution bulk crystal with a similar CdTe content (about 20%). The results of such comparison are presented in Fig. 5 and Fig. 6. Only a small difference of H and E values determined for both types of crystals is seen. A similar effect was reported for (Hg,Cd)Te solid solution containing 30% of CdTe [20]. Therefore, we conclude that much higher nanohardness value of MBE grown layers and that of bulk crystals, that were found recently for PbTe [9], was not observed in the case of (Hg,Cd)Te solid solution.

4. Conclusions

The (Hg,Cd)Te solid solution epilayers with chemical compositions corresponding to the vicinity of zero energy gap were grown by MBE on exactly oriented and slightly

misoriented (001)-GaAs wafers with thick CdTe buffers. The structures were characterized by XRD, SEM, and AFM. It was demonstrated that for the epitaxial, MBE growth of this solid solution the use of misoriented GaAs substrates is preferred, which is in an agreement with similar observations reported for several other II–VI type semiconductors. The nanohardness and Young's modulus determined for MBE grown layer were compared with respective values determined for the bulk crystal with the same chemical composition. Present results did not reveal any significant difference of obtained nanohardness values for both types of studied crystals, in contrast to that reported previously for PbTe.

Acknowledgments

This research was partially supported by the National Science Centre (Poland) through grant UMO-2014/13/B/ST3/04393 and by the Foundation for Polish Science through the IRA Programme co-financed by EU within SG OP.

References

- [1] R. Dornhaus, G. Nimtz, *Narrow Gap Semiconductors*, Vol. 98, Springer, Berlin 1985.
- [2] E. Kane, *J. Phys. Chem. Solids* **1**, 82 (1956).
- [3] W. Bardyszewski, W. Szuszkiewicz, Q. Dingrong, Z. Jiaming, *Acta Phys. Pol. A* **77**, 269 (1990)
- [4] E.M. Sheregii, J. Cebulski, A. Marcelli, M. Piccinini, *Phys. Rev. Lett.* **102**, 045504 (2009).
- [5] A. Rogalski, *Rep. Prog. Phys.* **68**, 10 (2005).
- [6] J. Chu, A. Sher, *Physics and Properties of Narrow Gap Semiconductors*, Springer, New York 2008.
- [7] G. Tomaka, J. Grendysa, M. Marchewka, P. Śliż, C.R. Becker, A. Stadler, E.M. Sheregii, *Opto-Electron. Rev.* **25**, 188 (2017).
- [8] M. König, H. Buchmann, L.W. Molenkamp, T. Hughes, C-X. Liu, X.L. Qi, S.C. Zhang, *J. Phys. Soc. Jpn.* **77**, 031007 (2008).
- [9] S. Adamiak, E. Łusakowska, E. Dynowska, R. Minikayev, P. Dziawa, A. Szczerbakow, W. Szuszkiewicz, *Phys. Status Solidi B*, **256** 1800549 (2019).
- [10] V. Klinger, T. Roesener, G. Lorenz, *Thin Solid Films* **548**, 358 (2013).
- [11] J. Grendysa, C.R. Becker, M. Trzyna, R. Wojnarowska-Nowak, E. Bobko, E.M. Sheregii, *EPJ Web Conf.* **133**, 01002 (2017).
- [12] J. Grendysa, G. Tomaka, P. Śliż, C.R. Becker, M. Trzyna, R. Wojnarowska-Nowak, E. Bobko, E.M. Sheregii, *J. Cryst. Growth* **480**, 1 (2017).
- [13] L. Śniadower, M. Psoda, R.R. Gałazka, *Phys. Status Solidi*, **28**, K121 (1968).
- [14] S. Miotkowska, I. Miotkowski, E. Dynowska, *Acta Phys. Pol. A* **86**, 737 (1994).
- [15] E. Janik, E. Dynowska, J. Bąk-Misiuk, M. Leszczyński, W. Szuszkiewicz, T. Wojtowicz, G. Karczewski, A.K. Zakrzewski, J. Kossut, *Thin Solid Films* **267**, 74 (1995).

- [16] J. Baars, F. Sorger, *Solid State Commun.* **10**, 875 (1972).
- [17] B.V. Robouch, A. Kisiel, E.M. Sheregii, *Phys. Rev. B* **64**, 073204 (2001).
- [18] J. Polit, E.M. Sheregii, J. Cebulski, A. Kisiel, A. Marcelli, B.V. Robouch, A. Mycielski, *Phys. Rev. B* **82**, 014306 (2010).
- [19] W. Szuszkiewicz, M. Jouanne, E. Dynowska, E. Janik, G. Karczewski, T. Wojtowicz, J. Kossut, W. Gebicki, *Semiconductor Heteroepitaxy: Growth, Characterization and Device Applications*, Eds. B. Gil, R.L. Aulombard, World Sci., Singapore 1995, p. 195.
- [20] M. Martyniuk, R.H. Sewell, C.A. Musca, J.M. Dell, L. Farone, *Appl. Phys. Lett.* **87**, 251905 (2005).
- [21] S. Cole, A.F.W. Willoughby, M. Brown, *J. Cryst. Growth* **59**, 370 (1982).
- [22] R. Triboulet, A. Lasbley, B. Toulouse, R. Granger, *J. Cryst. Growth* **79**, 695 (1986).
- [23] M. Schenk, A. Fissel, *J. Cryst. Growth* **86**, 502 (1988).
- [24] S. Fang, L.J. Farthing, M.-F.S. Tang, D.A. Stevenson, *J. Vac. Sci. Technol. A* **8**, 1120 (1990).
- [25] C.W. Myles, S.N. Ekpenuma, *J. Vac. Sci. Technol. B* **10**, 1454 (1992).
- [26] I.V. Kurilo, V.P. Alekhin, I.O. Rudyi, S.I. Bulychev, L.I. Osypshin, *Phys. Status Solidi A* **163**, 47 (1997).
- [27] R. Irwan, H. Huang, H.Y. Zheng, H. Wu, *Mater. Sci. Eng. A* **559**, 480 (2013).
- [28] R. Kuna, S. Adamiak, S. Petit, P. Baroni, K. Gas, R. Minikayev, A. Szczerbakow, J. Łażewski, W. Szuszkiewicz, *Acta Phys. Pol. A* **130**, 1245 (2016).
- [29] E. Łusakowska, S. Adamiak, P. Adamski, R. Kuna, R. Minikayev, P. Skupiński, A. Szczerbakow, W. Szuszkiewicz, *Acta Phys. Pol. A* **132**, 343 (2017).
- [30] C.M. Cube, *AIP Adv.* **6**, 095209 (2016).
- [31] K. Li, P. Yang, D. Xue, *Acta Mater.* **60**, 35 (2012).